Iran. J. Ichthyol. (2024) 11(2): 124-146
P-ISSN: 2383-1561; E-ISSN: 2383-0964

ORIGINAL ARTICLE

Insulin-like growth factor 1 (IGF1) in the hypothalamo-pituitary-gonadal-liver (HPG-L) axis: identification, sequencing, gene expression and in silico analysis in the Indian freshwater catfish, *Heteropneustes fossilis*

Uma Bharati SAHU[1], Kumari Vandana RANI[2], Neeta SEHGAL[*1]

[1]Department of Zoology, University of Delhi, Delhi, India.
[2]Department of Zoology, Kalindi College, University of Delhi, Delhi, India.

Correspondence
nsehgal@zoology.du.ac.in

Article history:
Accepted 27 May 2024

Abstract
Insulin-like growth factor 1 (IGF1) is involved in various physiological functions that are regulated by somatotropic (GH-IGF1) axis. To decipher the role of IGF1 in the HPG-L axis gene encoding *igf1* cDNA of female catfish, *Heteropneustes fossilis*, has been sequenced followed by in silico analysis as well as seasonal expression of *igf1* in brain, liver and ovary organs. The mRNA expression of *igf1* gene in these three organs elucidates that it plays a pivotal role in the HPG-L axis. In ovary, *igf1* gene expression exhibits a direct correlation with gonadosomatic index, whereas, an inverse relationship has been observed in brain and liver tissues. Hence upregulation of *igf1* in brain and liver, during the post-spawning phase and downregulation in ovary shows the shift from gonadal growth to somatic growth in resting phase. In silico analysis depicts that IGF1 is stable and hydrophilic in nature with 159 amino acid (aa) and molecular weight of 17.65 kDa. Secondary structure shows the presence of maximum random coils and alpha-helix. It is secretory protein showing maximum interaction with IGF1R, estrogen receptor alpha and GH. Protein structures of IGF1, luteinizing hormone beta (LHβ), follicle stimulating hormone beta (FSHβ) and growth hormone (GH) have been constructed and interaction among them has been docked which suggests that gonadal and somatic axes are probably interlinked and may regulate the neuroendocrine system of fish.

Keywords: Insulin-like growth factor 1 (IGF1), in silico analysis, Hypothalamo-pituitary-gonadal-liver (HPG-L) axis, Seasonal reproduction, *Heteropneustes fossilis*.

INTRODUCTION

Environmental cues photoperiod and temperature in addition to food availability play an important role in development of gonads in teleost. These external stimuli impinge on the external receptors, which send signals to the brain, where hypothalamus processes this information and regulates the neuroendocrine activity of the hypothalamic-pituitary-gonadal (HPG) axis and of somatotropic axis (Vasal & Sundararaj 1976; Levavi-Sivan et al. 2010; Zohar et al. 2010; Biran & Levavi-Sivan 2018). Hypothalamus in response to photoperiod and temperature signals produces neuropeptide gonadotropin releasing hormones (GnRH) which acts on the adenohypophysis of pituitary to release gonadotropins, follicle stimulating hormone (FSH) and luteinizing hormone (LH), which in turn control the synthesis of appropriate gonadal steroids in the gonads for the development and maturation of gametes. In fact, during reproduction, gonadal growth is the main focus of the fish. Therefore, the stored energy reservoirs are mainly diverted for the reproductive processes (Torre et al. 2014; Mcbride et al. 2015). Liver synthesizes an egg-yolk precursor protein, vitellogenin (a phospholipoglycoprotein) under the influence of estradiol-17β (E_2) in female fish (Lubzens et al. 2010; Hara et al. 2016). FSH controls synthesis and release of E2 from the ovarian follicle (Arukwe 2001; Nagahama & Yamashita 2008; Hollander-Cohen et al. 2021). Moreover, growth includes both somatic as well as gonadal growth along with energy metabolism. Under suitable conditions, growth hormone (GH) is released from the pituitary that acts on the liver to produce insulin like growth factor (IGF1). IGF1, a metabolic hormone, metabolizes carbohydrates, proteins and lipids in the targeted tissues, differentiates cells and finally leads to growth of the tissues (Moriyama et al. 2000). Hence, somatotropic axis, i.e., growth hormone and insulin-like growth factor 1 (GH-IGF1) axis regulates growth (Le Roith et al. 2001; Wood et al. 2005; Boan et al. 2024). This suggests that hormones for growth

and energy metabolism are likely to be involved in the reproductive pathway. Hence, in seasonal breeder teleost, development depends on the coordinated functionality of these two axes gonadotropic axis and somatotropic axis making it hypothalamus- pituitary-gonad- liver axis (HPGL- axis) wherein IGF1 play a pivotal role (Arukwe 2001; Hanson et al. 2021).

Insulin-like growth factors (IGFs) are evolutionarily highly conserved proteins throughout all the groups of vertebrates (Le Roith et al. 2001; Wood et al. 2005; Ndandala et al. 2022). The system consists of ligands (IGF1 and IGF2), high-affinity receptors, and their binding proteins. Later, in 2008, another ligand known as IGF3 restricted to teleost has been identified, which is mainly present in somatic cells of the gonads (Wang et al. 2008; Berishvili et al. 2010; Li et al. 2021). IGF1 regulates the neuroendocrine mechanism of growth and modulate the biological functions like differentiation, survival, growth, and metabolism through autocrine, paracrine, and endocrine mechanisms (Moriyama et al. 2000; Duan & Xu 2005; Wood et al. 2005; Duan et al. 2010; Qin et al. 2020). Growth hormone stimulates the production of IGF1 in liver as it is the principle source for its synthesis and its receptors are present in all the tissues therefore IGF1 is produced ubiquitously. Although, IGF1 is transported to other tissues from liver through the blood, but it may act in an autocrine and paracrine manner as well. The presence of IGF1 in the plasma and somatostatin negatively regulates GH, which implies the evolutionarily conserved neuroendocrine axis, the somatotropic axis (GH-IGF1) (Reinecke et al. 1997, 2005; Triantaphyllopoulos et al. 2020). IGF1 binds to the tyrosine kinase receptors (IGF1R), which are heterodimer containing a pair of alpha and beta subunits. Binding of the ligand leads to the autophosphorylation of downstream kinases, which stimulates the signaling cascades and various biological functions like glucose metabolism and mitogenesis (Jones 1995; Duan & Xu 2005; Duan et al. 2010; Ndandala et al. 2022).

Literature suggests that IGF1 helps in increasing the GnRH stimulated gonadotropic hormones both FSH and LH release from cultured pituitary cells under in vitro conditions in coho salmon (*Oncorhynchus kisutch*) and rainbow trout (*O. mykiss*) and zebrafish (*Danio rerio*) (Weil et al. 1999; Baker et al. 2000; Line & Ge 2009; Luckenbach et al. 2010). It also affects transcripts levels of gonadotropins in coho salmon (*Oncorynchus kisutch*) (Luckenbach et al. 2010). IGF1 promotes proliferation of follicular cells (medaka, *Oryzias latipes*) and increases oocyte size (short finned eel, *Anguilla anguilla*) in ovaries (Wood et al. 2005; Reinecke 2010; Lokman et al. 2007; Yuan et al. 2018). In addition, it promotes oocyte maturation in red seabream, mummichog and short-finned eel (Kagawa et al. 1994; Negatu at al. 1998; Lokman et al. 2007; Reinecke 2010; Yuan et al. 2018).

The Indian freshwater catfish, *Heteropneustes fossilis* is distributed throughout the Indian subcontinent has high protein and iron content but less fat. It has a high market value due to its medicinal and therapeutic properties, and is widely cultivated in the Indian subcontinent and an annual breeder fish spawns during the monsoon season. The reproductive cycle is divided into 4 phases: preparatory phase (February–April), pre-spawning phase (May–June), spawning phase (July–August), and post-spawning phase (September–January) (Goswami & Sundararaj 1968; Chaube et al. 2022; Pant et al. 2023). The present study focuses on the in silico analysis of IGF1 and its functional aspects in the catfish through protein modelling. Molecular and structural aspects of IGF1 are studied to understand the effect of IGF1 on the reproductive axis. Ontogenic studies have been performed to elucidate the molecular and biological functions. Gene expression of *igf1* has been evaluated in the brain, liver, and ovary throughout the reproductive cycle. An attempt has been made to study the crosstalk between the somatotropic and gonadotropic axes through docked structures of IGF1 with FSHβ, LHβ and GH. The present study also illustrates the active sites and binding interfaces involved in protein-protein interactions through computational tools.

Table 1. Semi-quantative and qPCR primers for *igf1* and *β-actin*.

Semi-quantitative PCR primers			
Transcript	Primer	Sequence (5'→3')	Amplicon Size (bp)
igf1	Forward	ATCCGTCTCCTGTCCGCTAAAT	632
	Reverse	GGCACTGTCCGATATTTCCAC	
β-actin	Forward	CTGGCCGTACCACAGGTATC	203
	Reverse	GATGTCACGCACGATTTCAC	
qPCR primers			
Transcript	Primer	Sequence (5'→3')	Amplicon Size (bp)
igf1	Forward	TGACTGTGACCAGAAGATAGAGGTT	132
	Reverse	CTGCGAGCTGAAGCGACT	
β-actin	Forward	GAGCACCCTGTCCTGCTTAC	136
	Reverse	GTACAGGGACAGCACAGCC	

MATERIALS AND METHODS

Animal maintenance and ethics statement: Adult specimens of catfish, *H. fossilis*, were collected from the backwaters of the river Yamuna in and around the National Capital Region of Delhi (Lat. 28º35´ N, Long. 77º12´E). Fish were acclimatized to the laboratory conditions for 7–10 days prior to use in the experiments. Fish were fed *ad libitum* and the water in the tanks was renewed on alternate days (Lamba et al. 1983). Specimens were euthanized with 0.001% phenoxyethanol, and tissues were collected for experimental procedures.

Isolation of *igf1* gene: The acclimated fish were decapitated, liver (50 mg) tissue was collected and homogenized to extract total RNA using the standardized protocol of the acid-guanidinium thiocyanate–phenol–chloroform extraction method (TRI Reagent, Sigma, T9424) (Chomczynski & Sacchi 2006). Concentration and quality of RNA was checked, then cDNA was synthesized and stored at -20ºC until use (Pipil et al. 2015). Degenerated primers specific for *igf1* were designed using the sequences of *igf1* from other vertebrate sequences retrieved from the NCBI database, and aligned by CLUSTALW using multiple sequence alignment (Table 1). cDNA of liver was used to amplify *igf1* gene using a semi-quantitative PCR method and the desired amplicon was electrophoresed and visualized on 1.2% agarose gel containing ethidium bromide stain. The gel was excised, and the desired product was eluted using the GeneJET gel extraction kit according to the manufacturer's protocol (Thermo Fisher Scientific, USA). The partial sequence obtained after Sanger sequencing of eluted product showed complete similarity with the nucleotide sequences of the *igf1*. The eluted product that contained the complete coding sequences (CDS) of *igf1* was submitted to the NCBI GenBank database (accession number: MN395400.1).

In silico analysis of IGF1: The identity of nucleotide sequences, was checked using the BLAST tool of NCBI (https://blast.ncbi.nlm.nih.gov/Blast.cgi?PROGRAM=blastn&BLAST_SPEC=GeoBlast&PAGE_TYPE=BlastSearch). Open Reading Frame (ORF) of the nucleotide sequence was obtained using the NCBI ORF Finder (https://www.ncbi.nlm.nih.gov/orffinder). ExPASY was used as a translation tool to deduce the protein sequence from the ORF (https://web.expasy.org/translate/). The protein sequence thus obtained was used for the in silico analysis. To identify the signal peptide in the protein, SignalP-5.0 was used (https://services.healthtech.dtu.dk/services/SignalP-5.0/). The protein sequences from other vertebrates were extracted from the database and aligned using the PRALINE multiple sequence alignment software (https://www.ibi.vu.nl/programs/pralinewww/).

Phylogenetic tree was constructed using the molecular evolutionary and genetic analysis version 7.0 (MEGA 7.0) software, in which protein sequences from various vertebrates (*Heteropneustes fossilis*,

QJI10543.1, *Tachysurus fulvidraco,* AKJ66813.1; *Pangasianodon hypophthalmus*, XP_034169274.1; *Tachysurus ussuriensis*, APF47229.1; *Labeo rohita*, AME16981.1; *Ctenopharyngodon idella*, AAF65819.1; *Hypothalmichthys molitrix*, AGH28092.1; *Hucho taimen,* ALF36868.1; *Xenopus laevis*, NP_001156865.1; *Gallus gallus*, NP_001004384.1; *Aligator sinensi*, ALQ12262.1; *Mus musculus*, AAL34535.1; *Homo sapiens*, AAI48267.2) were aligned using neighbor joining method and the gaps were completely deleted. A bootstrap value of 1000 was used for constructing the phylogenetic tree.

The secondary structure of the protein, IGF1 was deduced using SOPMA (https://npsa-pbil.ibcp.fr/cgi-bin/npsa_automat.pl?page=/NPSA/npsa_sopma.html) and PSIPRED (http://bioinf.cs.ucl.ac.uk/psipred/). Parameters like isoelectric point, molecular weight, amino-acid composition along with the negative and positive amino acid residues, extinction coefficient, half-life, instability index, aliphatic index, and the grand average of hydropathicity (GRAVY) was predicted using the ProtParam tool of ExPASY (https://web.expasy.org/protparam/). Gene ontology was predicted for biological process, molecular function, and cellular component, and subcellular localization of the protein was deduced using PSIPRED and CELLO2GO (http://cello.life.nctu.edu.tw/cello2go/) software respectively. Phosphorylation sites at serine, threonine, and tyrosine were found using the online server NetPhos3.1 (https://services.healthtech.dtu.dk/services/NetPhos-3.1/). Protein –protein interaction of IGF1 with other proteins involved in the HPG axis was predicted using the online STRING software tool (https://string-db.org).

Predication of 3D structures of IGF1, LHβ, FSHβ and GH and their validation: The three-dimensional structure of IGF1, LHβ, FSHβ and GH were predicted using Iterative Threading Assembly Refinement (I-TASSER) server (https://zhanggroup.org/I-TASSER/). Top five models for each protein sequence were generated and the best model was selected on the basis of confidence score (C-score) and threading sequence identity (Zhang 2008; Roy et al. 2010). Structures were visualized using PyMOL by Schrödinger (https://www.pymol.org/). The top structures were bought to energy minimization without changing or fixing any of their atoms for structural refinement using the YASARA energy minimization server (https://www.yasara.org/minimizationserver.htm) (Krieger et al. 2009). After energy minimization, the structures were validated for their stereochemical quality by Ramachandran plot created using PROCHECK (https://saves.mbi.ucla.edu/). The coarse packing quality of the minimized energy models was checked using the WHAT IF server (https://swift.cmbi.umcn.nl/servers/html/index.html). The non-bonded interaction among the atoms of the structures was determined by the ERRAT server (https://saves.mbi.ucla.edu/). The fold reliability in the protein structures was validated using X-ray and NMR spectroscopic structural validation using the ProSA-web server (https://prosa.services.came.sbg.ac.at/prosa.php) (Wiederstein & Sippl 2007; Messaoudi et al. 2013).

Binding site assessment and docking: The active binding sites of the proteins, were deduced using the Computed Atlas of Surface Topography of proteins (CASTp) server to identify and quantify the pockets (http://sts.bioe.uic.edu/castp/index.html?1bxw). Amino-acid residues involved in protein-protein interaction were found using a prediction interface called the CPORT algorithm, which provides the consensus prediction of interface residues in transient complexes (https://alcazar.science.uu.nl/services/CPORT/). Using the already available predicted protein interfaces in ambiguous interaction restraints (AIRs), docked complexes of protein structures for IGF1-LHβ, IGF1-FSHβ and IGF1-GH were produced using the High Ambiguity Driven protein-protein DOCKing (HADDOCK2.2) server (https://wenmr.science.uu.nl/haddock2.4/submit/1). HADDOCK produced models were organized into different clusters. The top 10 docked complexes were selected based on the HADDOCK score and z-score

for structural analysis of clusters. The protein-protein interaction in the docked complexes was analyzed using the Proteins, Interfaces, Structures, and Assemblies (PDBePISA) server of the PDB (for details refer to Kumari et al. 2020).

Expression analysis of *igf1* gene: Fish were collected once every month for a period of one year for annual profiling of *igf1* gene expression. Fish (n=6) was weighted and decapitated, ovaries were dissected and weighed to calculate the gonado-somatic index (GSI). In addition, whole brain and 50mg of each tissue (liver and ovary) was homogenized to extract total RNA. The integrity of the isolated RNA was assessed through absorbance A260/280, followed by the cDNA synthesis (Pipil et al. 2015).

Gene expression levels of *igf1* in brain, liver and ovary was determined by RT-PCR. Gene expression was quantified using the power SYBRTM Green PCR master mix (Thermo Fisher Scientific, USA). qPCR primers for *igf1* and *β-actin* was synthesized from the conserved regions of both the genes (Table 1). The amplification was carried out in 10µL of total reaction volume in 384 well, QuantStudio 6 Flex applied biosystem (Kumari et al. 2021). *β-actin* was taken as calibrator. The relative fold change of *igf1* was quantified using the $2^{-\Delta\Delta Ct}$ method (Livak & Schmittgen 2001). The PCR efficiency of primers was within the range of 95%- 110%. The data obtained was analyzed by QuantStudioTM Real-Time PCR software (v1.7.2). Statistical analysis was done using IBM®SPSS 23.0 software. All data are represented as mean±SEM. Data was compared using one-way ANOVA followed by Duncan's multiple post hoc range (P<0.05).

RESULTS

In silico analysis of IGF1: The ORF obtained from the nucleotide sequence of 632 bp was 480 bp long, translating a putative protein of 159 amino acids (Fig. 1a). The amino acid sequence has six conserved cysteine residues and can be divided into 5 domains: B (29 aa), C (12 aa), A (21 aa), D (9 aa), and E (47aa). Further, B has two (Cys^{B6} and Cys^{B18}) and A has four (Cys^{A6}, Cys^{A7}, Cys^{A11}, Cys^{A20}) conserved cysteine residues (Fig. 1a). The signal peptide was 41 aa long (Fig. 1b). The protein is secretory in nature with maximum likelihood score of 0.9753. Multiple sequence alignment of amino acid sequences of IGF1 among vertebrates showed that it has the conserved insulin family signature sequence. This conserved sequence (CCFQSCELKRLEMYC) was found to be 15 aa long (from 88 aa to 102 aa) (Fig. 2). Phylogenetic tree analysis suggests that the aa sequence of IGF1 is highly similar to the IGF1 sequences of the teleost belonging to order siluriformes (Fig. 3).

The secondary structure of IGF1, predicted using SOPMA and PSIPRED software, has been shown in Fig. 4. It elucidates that the sequence contains maximum random coil (84 aa, 52.83%), followed by alpha-helix (57 aa, 35.85%), and minimum extended strands (12 aa, 7.55%), and beta turns (6 aa, 3.77%).

The physicochemical parameters were computed using the ProtParam software (Table 2). The predicted molecular weight of IGF1 was 17.66 KDa with an isoelectric point (pI) of 9.92. The protein contains maximum arginine (10.1%), followed by leucin and glycine (9.4% each). The instability index was 36.71, which suggests that the protein is stable. The aliphatic index and GRAVY index were computed as 63.14 and -0.560, respectively.

The gene ontology of the protein was predicted using PSIPRED and CELLO2GO software, and it was found to be extracellular in nature with maximum score value of 3.885 (Fig. 5). The gene ontology was predicted with the help of the maximum probability score and support vector machines (SVM) reliability index which suggests that IGF1 is involved in biological processes like cell surface receptor signaling pathways, regulation of metabolic processes, transport, regulation of nitrogen compound metabolic processes, G-protein coupled receptor signaling pathway, ion transport, regulation of gene expression etc. (Table 3). The protein also showed a higher SVM and probability score for molecular functions which suggest that the protein is involved in G-protein coupled receptor binding, nucleic acid binding, sequence-specific DNA binding transcription

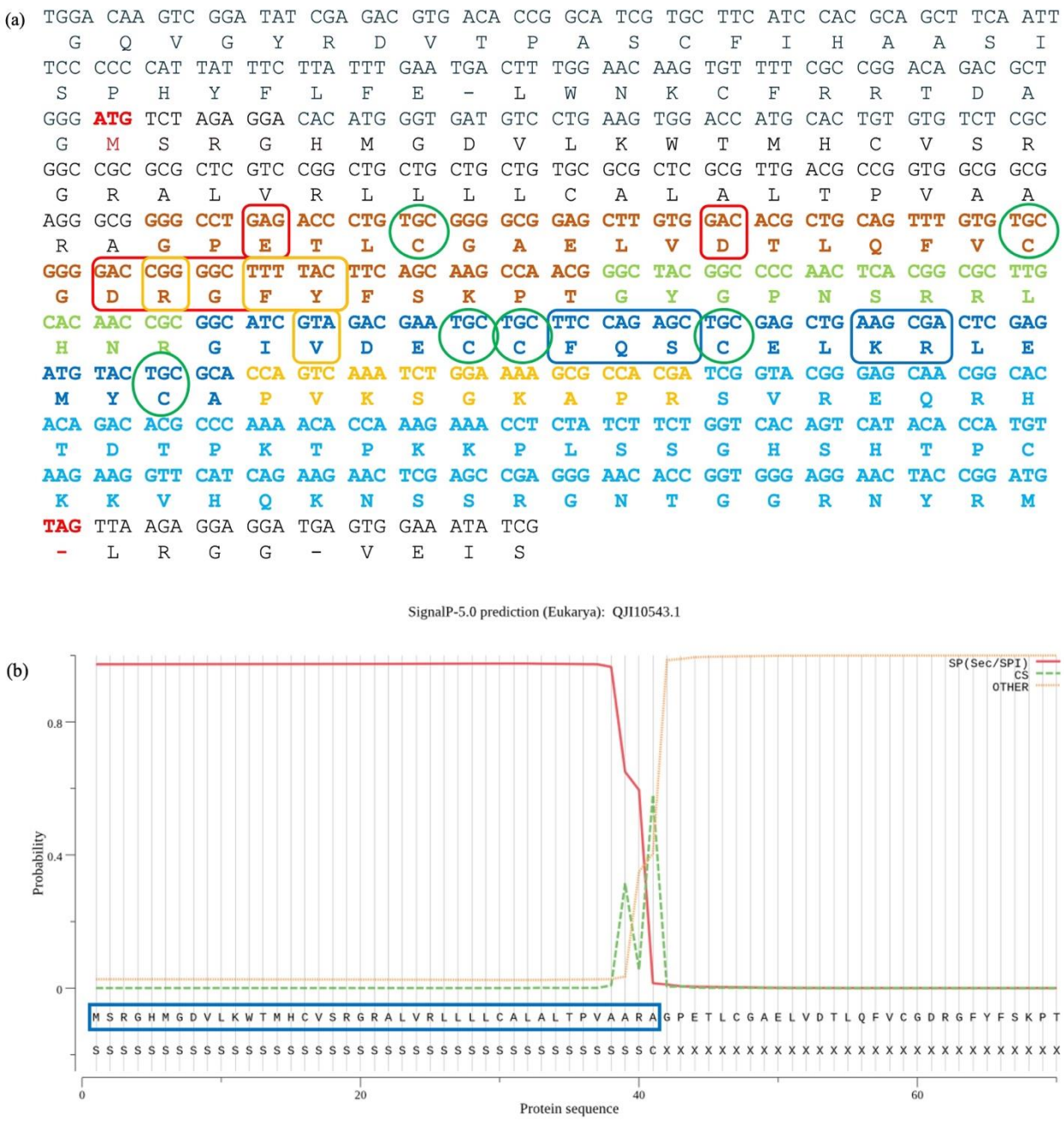

Fig.1. (a) In silico translation of nucleotide sequence of *igf1* into coding sequence (CDS). Start and stop codons are highlighted in red. Insulin-like growth factor binding protein binding sites on IGF1 are enclosed in red box. Type 1 IGF receptor binding surface are enclosed in yellow box. Type 2 IGF receptor binding surface are enclosed in blue boxes. 6 conserved cysteine residues are enclosed in green box. B, C, A, D and E domains are highlighted in brown, green, dark blue, yellow and blue color respectively. (b) Signal peptide of 41 amino acids is enclosed in blue box, cleavage site between 41 and 42 i.e., between ARA- GPE.

factor activity, enzyme inhibitor activity etc.

Phosphorylation sites in IGF1 occurred at various sites (serine, threonine, and tyrosine) with protein kinase C (PKC) activity at 120th and 147th positions, cyclin-dependent kinase inhibitor (CKI) activity at the 67th position, and epidermal growth factor receptor (EGFR) kinase activity at the 72nd position. There are other unspecific phosphorylation activities at the 18th, 35th, 45th, 107th, 113th, 122nd, 125th, 131st, 132nd, 135th, 137th, 148th and 152nd positions (Fig. 6, Table 4).

Possible protein-protein interaction of IGF1 with other proteins that are predicted to be involved in HPG axis was found with tyrosine-protein kinase receptor, insulin-like growth factor 1b receptor (IGF1Rb) with

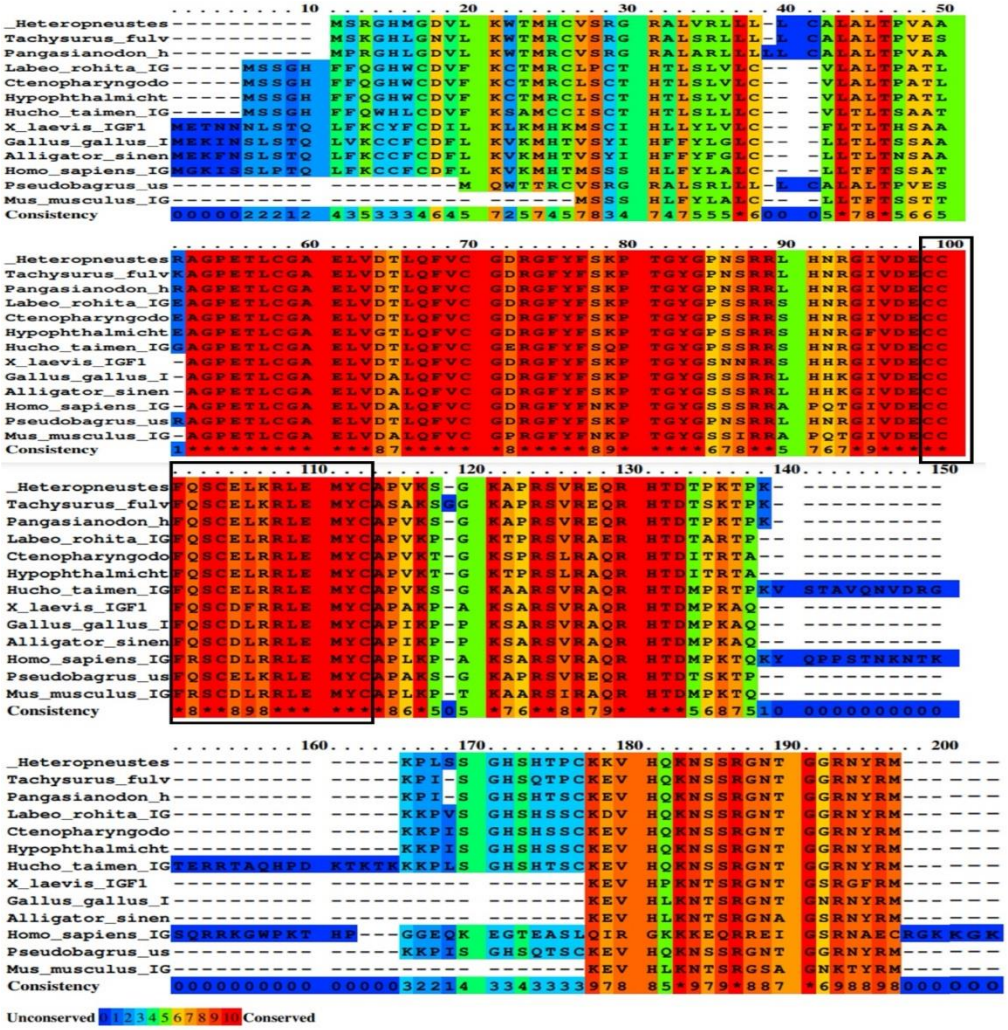

Fig.2. Amino acid sequence of IGF1 of different vertebrates are aligned. Insulin family conserved sequence in all the vertebrate groups is enclosed in black box. Degree of conservation is shown according to the numeric values where 0 is the lowest and 10 is the highest.

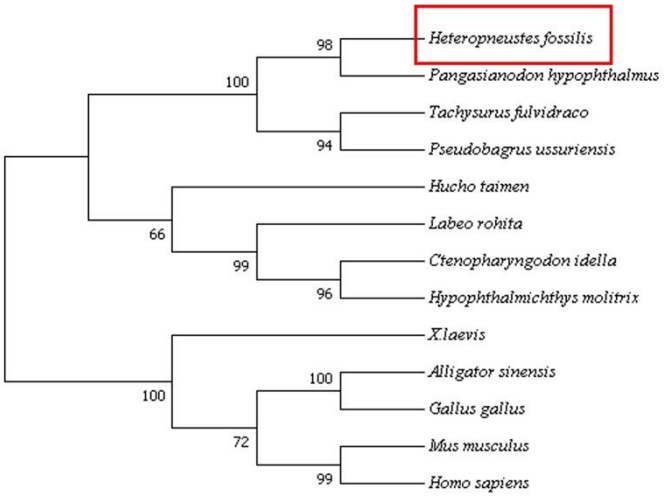

Fig.3. Phylogenetic tree constructed using IGF1 amino acid sequences from different vertebrates. The phylogenetic analysis was done using maximum-likelihood tree, and to assess the robustness, a bootstrap value of 1000 replicates was considered. The values represented on the branches depict the percentage of replicate trees clustered together to form the same taxa.

maximum confidence score of 0.999, and minimum with mitogen-activated protein kinase 12 (mapk12a) with a confidence score of 0.427 (Fig. 7, Table 5).

Prediction 3D structures of IGF1, LHβ, FSHβ and GH and their validation: I-TASSER was used to build the protein models for IGF1, LHβ, FSHβ and GH. From top five models generated by the software, the best model was selected on the basis of confidence score (C-score) and template modelling score (TM-score) (Fig. 8a). The c-score and tm-score of IGF1, LHβ, FSHβ and GH are mentioned in table 7. The models were then submitted for energy minimization in the YASARA force field, and the resultant energies and scores obtained after minimization were 65954.1 kJ/mol, -5.13; -47779.7 kJ/mol, -2.43; -46791.4 kJ/mol, -2.45 and -78005.0 kJ/mol, -4.59 for IGF1,

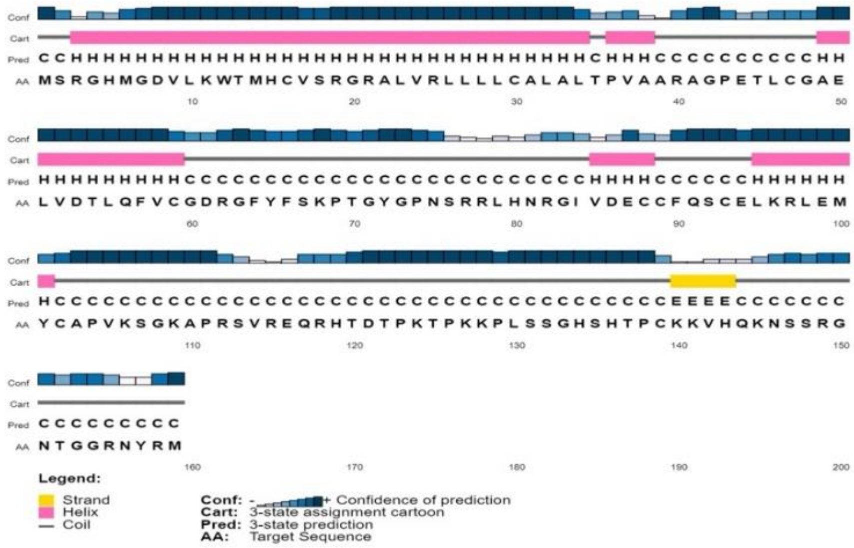

Fig.4. Secondary structure of IGF1 is predicted using PSIPRED software (H: Helix, C: Random coils, E: Extended strand).

Table 2. Physiochemical parameters of IGF1 identified using ProtParam software.

S. No.	Parameters	Number
1	Number of amino acids	159
2	Molecular weight	17656.45
3	Theoretical pI	9.92
4	Total number of negatively charged residues (Asp + Glu)	11
5	Total number of positively charged residues (Arg + Lys)	27
6	Total number of atoms	2463
7	Extinction coefficient	11960 M^{-1} cm^{-1}
8	Instability index	36.71 (stable)
9	Aliphatic index	63.14
10	Grand average of hydropathicity (GRAVY)	-0.560

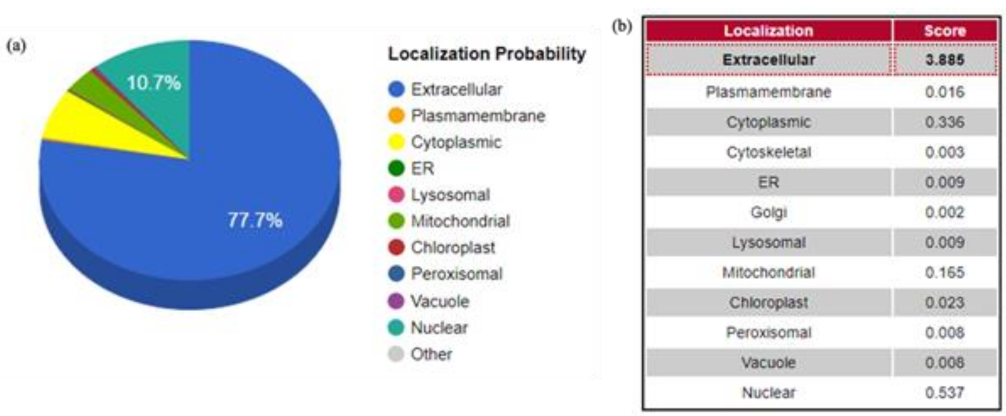

Fig.5. Representation of cellular localization of IGF1 in (a) pie chart and (b) tabular form.

LHβ, FSHβ and GH respectively. The Ramachandran plot produced by PROCHECK shows the presence of torsional angles (psi and phi) of amino acid residues of the protein in allowed and disallowed regions, which indicates the quality of the protein 3-D model. Results show that 90.1%, 94.2%, 98.3% and 96.7% residues of IGF1, LHβ, FSHβ and GH, respectively are present in the most favored and allowed regions (Fig. 8b, Table 6). 6.8%, 2.5%, 0.9% and 0.5% residues of IGF1, LHβ, FSHβ and GH respectively are present in generously allowed regions, and 3.0%, 3.3%, 0.9% and 2.7% residues of IGF1, LHβ, FSHβ

Table 3. Prediction of biological and molecular functions of IGF1.

S.No.	Biological Process	Probability	SVM Reliability
1	cell surface receptor signaling pathway	0.901	H
2	regulation of metabolic process	0.870	H
3	Transport	0.790	H
4	regulation of nitrogen compound metabolic process	0.735	H
5	G-protein coupled receptor signaling pathway	0.671	H
6	ion transport	0.668	H
7	regulation of gene expression	0.633	H
8	macromolecule biosynthetic process	0.630	H
	Molecular Functions		
1	G-protein coupled receptor binding	0.805	H
2	nucleic acid binding	0.582	H
3	sequence-specific DNA binding transcription factor activity	0.572	H
4	enzyme inhibitor activity	0.501	H
5	signal transducer activity	0.545	H
6	cytokine activity	0.853	H
7	cytokine receptor binding	0.589	H
8	growth factor activity	0.612	H

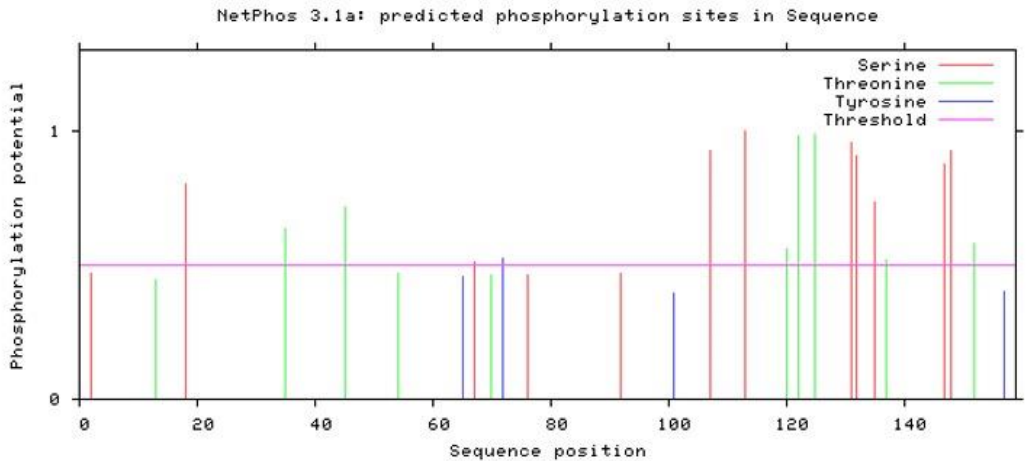

Fig.6. Phosphorylation sites are depicted with serine, threonine and tyrosine are shown in red, green and blue respectively. Threshold (0.5) is shown with pink.

and GH respectively are present in disallowed regions, which suggests that the backbone of predicted models are stereochemically stable. The z-score of the Ramachandran plot and score by WHATIF server were -5.714 and -2.377 for IGF1; -3.570 and -2.295 for LHβ; -2.937 and -2.079 for FSHβ and -2.477 and -0.357 for GH respectively which suggests that the predicted models are of good quality. ERRAT scores for IGF1 was 84; 85.95 for LHβ; 90.74 for FSHβ, and 96.2963 for GH (Table 7). The z-scores obtained from ProSA web were -3.77 for IGF1, -3.56 for LHβ, -5.2 for FSHβ and -5.96 for GH (Fig. 8c).

Binding site assessment and docking: Amino acid residues involved in pocket or void formation required for binding of proteins for IGF1, LHβ, FSHβ and GH were computed using the CASTp server (Table 8). The active amino acid residues which are involved in protein-protein interaction were obtained from CPORT and subjected to the HADDOCK server to produce docked structures of protein complexes

Table 4. Amino acid positions of phosphorylation with their predicted kinases in IGF1 protein.

Phosphorylation site	Kinase
67th serine	CKI
72nd tyrosine	EGFR
120th threonine	PKC
147th serine	PKC

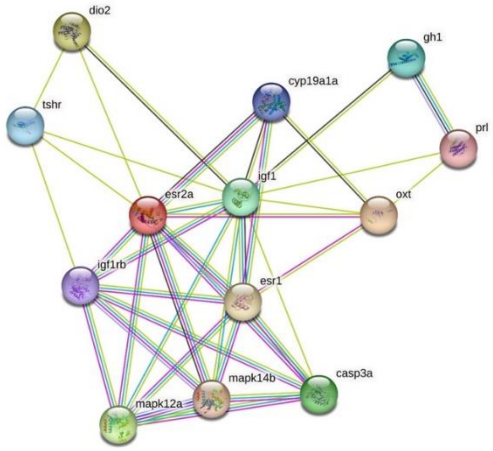

Fig.7. Protein-protein interactions of IGF1 with proteins that are involved in hypothalamo- pituitary- gonad axis predicted by STRING software.

Table 5. Protein-protein interaction of IGF1 with other proteins depicted in score provided by STRING software**.**

Protein	Protein Annotation	Score
IGF1RB	Tyrosine-protein kinase receptor; Insulin-like growth factor 1b receptor	0.999
ESR1	Estrogen receptor alpha; The steroid hormones and their receptors are involved in the regulation of eukaryotic gene expression and affect cellular proliferation and differentiation in target tissues	0.963
ESR2A	Estrogen receptor beta2; Estrogen receptor 2a	0.764
GH1	Somatotropin precursor; Growth hormone 1	0.742
MAPK14B	Mitogen-activated protein kinase 14b; Serine/threonine kinase which acts as an essential component of the MAP kinase signal transduction pathway.	0.604
CYP19A1A	Aromatase; Catalyzes the formation of aromatic C18 estrogens from C19 androgens	0.585
CASP3A	Caspase 3, apoptosis-related cysteine protease a; Belongs to the peptidase C14A family	0.582
PRL	Prolactin	0.529
OXT	Oxytocin-neurophysin 1 precursor; Oxytocin; Belongs to the vasopressin/oxytocin family	0.514
TSHR	Thyrotropin receptor	0.482
DIO2	Type ii iodothyronine deiodinase; Responsible for the deiodination of T4 (3,5,3',5'-tetraiodothyronine)	0.469
MAPK12A	Mitogen-activated protein kinase 12; Serine/threonine kinase which acts as an essential component of the MAP kinase signal transduction pathway.	0.427

(Table 9). HADDOCK clustered 138 structures into 16 clusters, which represent 69% of the water refined model of the IGF1-FSHβ docked complex and 131 structures into 17 clusters, which represent 65% of the water refined model for IGF1-LHβ protein-protein interaction. In the case of IGF1-GH protein-protein interaction, HADDOCK clustered 114 structures into 18 clusters, representing 56% of the water refined

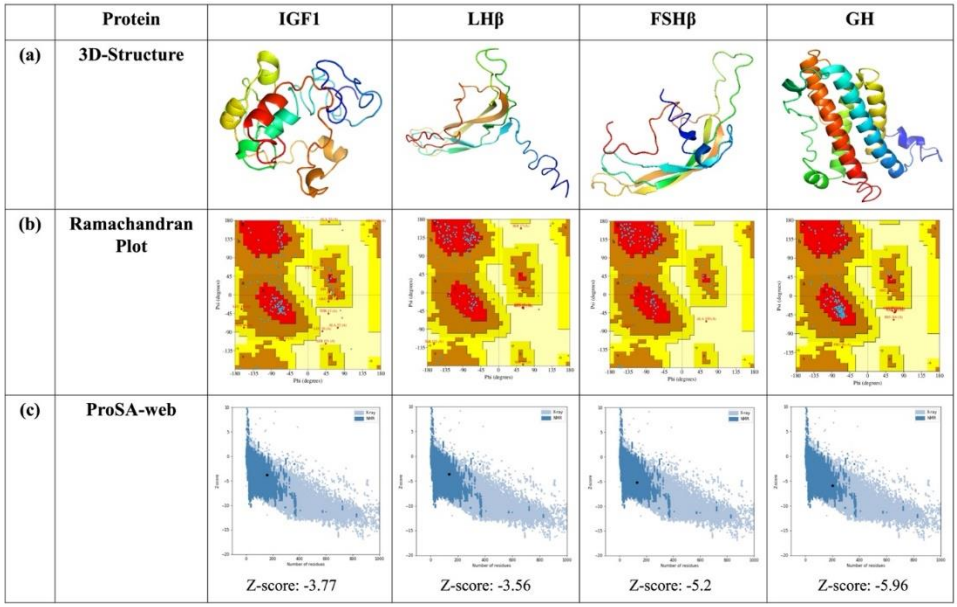

Fig.8. (a) 3-D structure of IGF1, LHβ, FSHβ and GH. (b) Ramachandran plot displaying the dihedral angles Psi and Phi of the amino acid residues of IGF1, LHβ, FSHβ and GH using PROCHECK software. (c) Z-score of the IGF1, LHβ, FSHβ and GH predicted by ProSA web server.

Table 6. Ramachandran plot statistics of amino acid residues of IGF1, LHβ, FSHβ and GH. Proteins having >90% amino acid residues in most favored and additional allowed regions and generously allowed regions are considered to be highly stable.

Plot Statistics	IGF1 (%)	LHβ (%)	FSHβ (%)	GH (%)
Residues in most favored and additional allowed regions	90.1	94.2	98.3	96.7
Residues in generously allowed regions	6.8	2.5	0.9	0.5
Residues in disallowed regions	3.0	3.3	0.9	2.7

Table 7. Quality analysis of IGF1, LHβ, FSHβ and GH.

Protein model	C-score	TM-score	Ramachandran z-score	WHATIF score	ERRAT score
IGF1	-3.40	0.37±0.13	-5.714	-2.377	84
LHβ	-2.63	0.62±0.14	-3.570	-2.295	85.95
FSHβ	-1	0.65±0.13	-2.937	-2.079	90.74
GH	-1.90	0.7±0.12	-2.477	-0.357	96.2963

models generated by HADDOCK (Fig. 9). The top 10 reliable clusters using the z-score were selected for all the docked complexes. Lower z-score indicates more trustworthy model. Out of these top ten models, cluster 16 with HADDOCK score of -75.4+/-8.0, electrostatic energy of 209.2+/-13.9 Kcal/mol and z-score of -2.0 considered as the most reliable IGF1-FSHβ docked complex whereas cluster 2 with HADDOCK score of -114.6+/-5.2, electrostatic energy of -288.1+/-64.4 and z-score value of -2.4 was considered to be most reliable IGF1-LHβ docked complex. Cluster 5 with a HADDOCK score of -66.9+/-5.5, electrostatic energy of -128.5+/-27.0 Kcal/mol and z-score of -2.1 was considered the reliable docked complex in the case of IGF1-GH. Amino acid residues involved in protein-protein interaction within the docked complexes were analyzed using the PDBePISA server. The interface area was computed as 1175.6 $Å^2$ and the free solvation gain energy (Δ^iG) was calculated as -17.8 kcal/M for IGF1-FSHβ docked complex whereas, IGF1-LHβ docked complex has an interface area of 1228.2 $Å^2$

Table 8. Area and volume of the pockets / binding sites assessed using CASTp server.

Protein Model	Binding residues	Area (Å^2)	Volume (Å^3)
IGF1	5 His, 6 Met, 8 Asp, 11 Lys, 19 Arg, 27 Leu, 40 Arg, 41 Ala, 42 Gly, 43 Pro, 49 Ala, 50 Glu, 52 Val, 53 Asp, 62 Arg, 63 Gly, 64 Phe, 65 Tyr, 105 Val, 110 Ala, 111 Pro, 112 Arg, 114 Val, 115 Arg, 119 His, 120 Thr, 121 Asp, 122 Thr, 123 Pro, 128 Lys, 130 Leu, 131 Ser, 132 Ser, 133 Gly, 134 His, 136 His, 139 Cys, 144 Gln, 158 Arg, 159 Met	498.612	303.074
LHβ	1 Met,2 Pro,3 Gly,4 Ser,6 Phe,7 Leu,8 Leu,9 Leu,10 Phe,11 Phe,12 Phe,13 Ile,14 Asn,15 Phe,16 Phe,17 Ser,18 Pro,19 Ala,20 Gln,21 Ser,22 Tyr,23 Leu,24 Leu,25 Thr,26 His,27 Cys,28 Gln,29 Pro,30 Val,31 Asn,32 Glu,33 Thr,34 Val,35 Ser,36 Val,37 Glu,38 Lys,39 Asp,40 Gly,41 Cys,42 Ser,43 Lys,44 Cys,45 Leu,46 Val,47 Phe,48 Gln,49 Thr,50 Ser,51 Ile,52 Cys,53 Ser,54 Gly,55 His,56 Cys,57 Phe,58 Thr,59 Lys,60 Glu,70 Ile,71 Tyr,72 Gln,73 His,74 Val,75 Cys,76 Thr,77 Tyr,78 Arg,79 Asp,80 Val,81 Arg,82 Tyr,83 Glu,84 Thr,85 Ile,86 Arg,87 Leu,88 Pro,89 Asp,90 Cys,91 Arg,92 Pro,93 Gly,94 Val,95 Asp,96 Pro,97 His,98 Val,99 Thr,100 Tyr,101 Pro,102 Val,103 Ala,104 Leu,105 Ser,106 Cys,107 Glu,108 Cys,109 Ser,110 Leu,111 Cys,112 Thr,113 Met,114 Asp,115 Thr,116 Ser,117 Asp,118 Cys,119 Thr,120 Ile,121 Glu,122 Ser,123 Leu,124 Asn,125 Pro,126 Asp,127 Phe,128 Cys,129 Met,130 Thr,131 Gln,132 Lys,134 Phe,135 Ile,136 Leu,137 Asp,138 Tyr	5271.788	4342.909
FSHβ	3 Arg,5 Val,6 Ala,7 Met,9 Leu,10 Leu,13 Met,30 Ile,32 Ile,47 Thr,48 Thr,49 Ala,50 Cys,51 Ala,52 Gly,53 Leu,54 Cys,56 Thr,70 Gln,71 Asn,72 Thr,73 Cys,74 Asn,75 Phe,99 Pro,100 Val,101 Ala,109 Cys,110 Asn,113 Ile,114 Thr,115 Asp,116 Cys,117 Gly,118 Ala,119 Phe,120 Ser,123 Pro	558.407	597.379
GH	35 CYS, 40 ASN, 51 TYR, 52 GLN, 53 CYS, 55 GLY, 56 CYS, 57 CYS, 59 SER, 60 ARG, 61 ALA, 62 TYR, 63 PRO, 65 PRO, 66 LEU, 67 ARG, 69 LYS, 70 LYS, 71 THR, 72 MET, 73 LEU, 74 VAL, 78 ILE, 79 THR, 80 SER, 81 GLU, 82 ALA, 83 THR, 84 CYS, 85 CYS, 86 VAL, 87 ALA, 90 VAL, 92 ARG, 98 VAL, 99 LYS, 100 LEU, 101 VAL, 103 HIS, 110 THR, 111 CYS, 112 TYR, 113 TYR, 114 HIS, 116 PHE	759.267	1228.437

Table 9. Active residues involved in protein-protein interaction among the proteins predicted by CPORT software.

IGF1	1, 2, 8, 12, 13, 14, 15, 16, 17, 18, 19, 20, 21, 23, 24, 25, 26, 28, 30, 31, 32, 33, 34, 35, 37, 38, 39, 44, 45, 74, 75, 77, 89, 90
FSHβ	1, 2, 3, 4, 5, 6, 7, 8, 9, 10, 11, 12, 13, 14, 15, 16, 18, 19, 21, 29, 30, 31, 44, 51, 52, 122, 123, 124, 125
LHβ	1, 2, 3, 4, 5, 6, 7, 9, 10, 11, 12, 13, 14, 15, 16, 17, 18, 19, 20, 21, 22, 23, 24, 25, 26, 28, 30, 54, 55
GH	1, 2, 3, 4, 5, 6, 7, 8, 9, 11, 12, 13, 14, 15, 16, 17, 18, 19, 20, 22, 23, 24, 25, 62, 126, 129, 130, 136, 137

with a free solvation gain energy ($\Delta^i G$) of -14.7 kcal/M. The interface area of the docked IGF1-GH complex was found to be 1107.7 Å^2, and the free solvation gain energy was 14.1kcal/mol (Table 10). Both hydrogen bonds and salt bridges were used for protein-protein interaction in the IGF1-LHβ and IGF1-GH docked complexes whereas only hydrogen bonds were present in the IGF1-FSHβ protein docked complex (Table 11 a, b and c).

Expression of *igf1* in brain, liver and ovary: The gonadosomatic index started increasing gradually during the preparatory phase and more rapidly during pre-spawning phase (May-June) and reached a peak in July-August. Thereafter, there was a sharp decline in GSI during spawning phase which remained low throughout the post-spawning phase (Fig. 10a). A sharp increase in the transcript levels of *igf1* in ovary was observed during the preparatory phase and peak was attained in April. High transcripts of *igf1* mRNA was maintained throughout pre-spawning phase.

Iran. J. Ichthyol. (2024) 11(2): 124-146

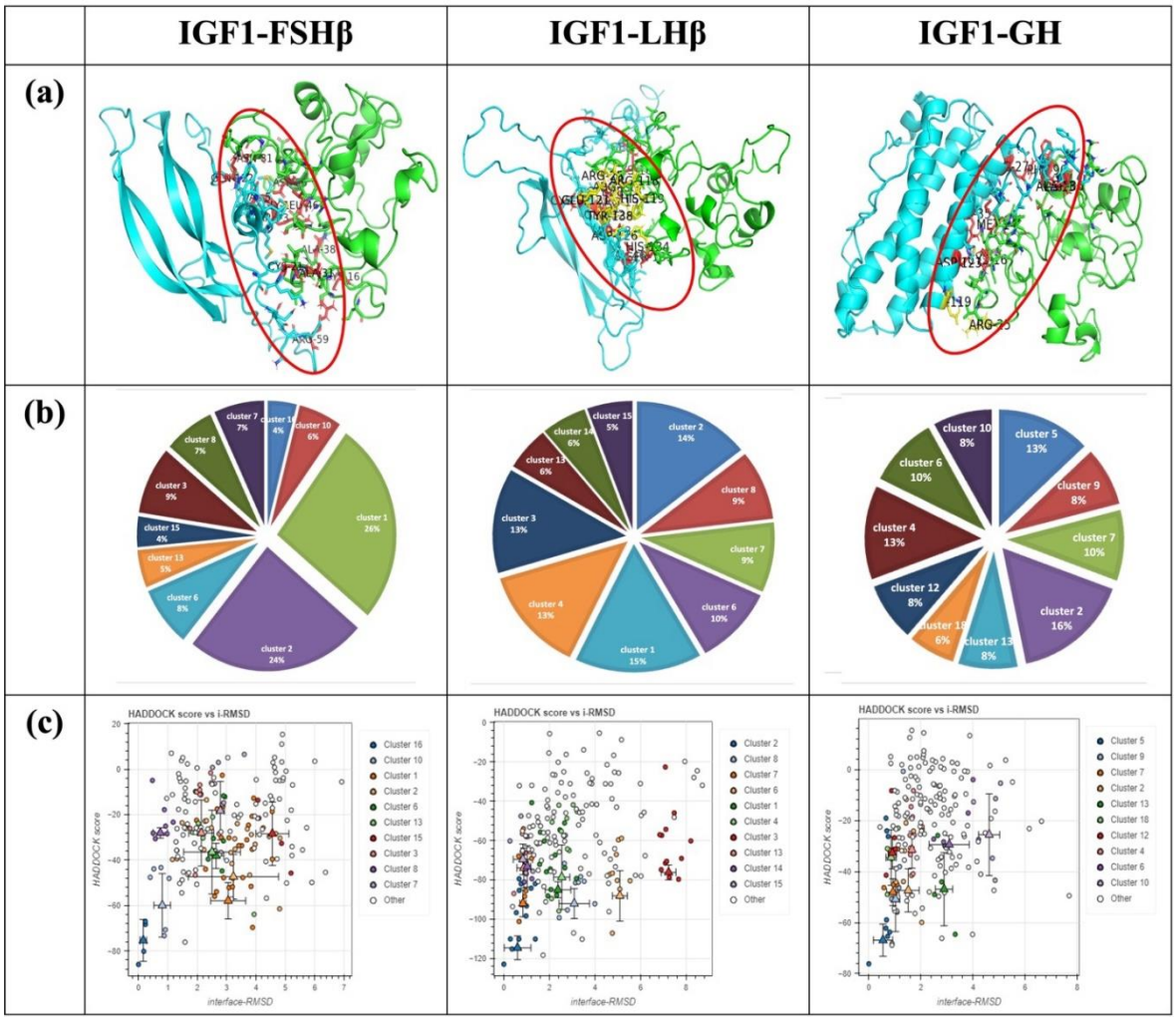

Fig.9. HADDOCK cluster analysis. (a) Diagrammatic illustration of best docked complex of IGF1–FSHβ, IGF-LHβ and IGF1-GH, where IGF1 shown in green and FSHβ, LHβ and GH are shown in blue, respectively. (b) Pie chart showing the HADDOCK cluster distribution with cluster size. (c) HADDOCK score plotted against their i-RMSD. The i-RMSD value of all 10 HADDOCK clusters are represented in different colors.

Transcripts of *igf1* declined during spawning phase, and remained low during the postspawning phase (Fig. 10c). The pattern of transcripts level of *igf1* in brain and liver was opposite to the one observed in ovary. mRNA of *igf1* was highest during the early preparatory phase and it declined sharply and remained low during the late preparatory and pre-spawning phases. The expression commenced during the spawning phase and reached its maximum during the post-spawning phase (Fig. 10 b & d).

DISCUSSION

The in silico analysis in the present study reveals that nucleotide sequence of *igf1* gene has 632 bp containing 480 bp long ORF encoding 159 aa and 41 aa long signal peptide. The deduced amino acid sequence has shown high sequence similarity with the siluriformes (90% with *Tachysurus fulvidraco* and 91.25% with *Pangasianodon hypophthalmus*). The presence of five domains (B, C, A, D, and E) and conserved cysteine residues on B and A domain in the catfish is in conformity with other teleost (Hober et al. 1997; Denley et al. 2005; Philippou et al. 2014; Nipkow et al. 2018). These two domains B and A are highly conserved and form disulfide bonds, providing stability to the tertiary structure and contain the binding sites of receptors and binding proteins (Magee et al. 1999). In *Oryzias latipes*, the *igf1* gene has 558 bp long ORF encoding 185 amino acid residues (Yuan et al. 2018), and the ORF of the tropical damselfish,

Table 10. IGF1-FSHβ, IGF1-LHβ and IGF1-GH interacting interface predicted by PDBePISA web server. iNat: number of interfacing atoms, iNres: number of interfacing residues, surface (A^{o2}): total solvent accessible area. Interface area (A^{o2}): difference in the total accessible surface area of isolated and interfacing structures divided by 2, Δ^iG (kcal/mol): solvation-free energy gain upon formation of the interface, Δ^iG P value: P value of the observed solvation-free energy gain, N_{HB}: number of hydrogen bonds, N_{SB}: number of salt bridges.

$^iN_{at}$	$^iN_{res}$	Surface Å^2	$^iN_{at}$	$^iN_{res}$	Surface Å^2	Interface area (Å^2)	Δ^iG kcal/ mol	Δ^iG P-value	N_{HB}	N_{SB}
	IGF1			FSHβ			IGF1-FSHβ			
123	36	9762	115	29	9533	1175.6	-17.8	0.211	13	0
	IGF1			LHβ			IGF1-LHβ			
109	28	9957	124	39	10938	1228.2	-14.7	0.358	14	14
	IGF1			GH			IGF1-GH			
99	31	9888	103	27	11466	1107.7	-14.1	0.147	6	4

Table 11. Analysis of hydrogen bonds and salt bridge interactions among the amino acid residues participating in (a) Interactions between IGF1-FSHβ.

Hydrogen bonds			
S. No.	IGF1	Dist. [Å]	FSHβ
1	ASN 81[N]	3.04	GLN 122[OE1]
2	ASP 86[OD1]	3.08	ARG 3[N]
3	ASP 86[OD2]	3.31	ARG 3[N]
4	LEU 46[O]	2.45	ARG 3[HE]
5	ALA 38[O]	2.41	ARG 3[HH12]
6	ALA 38[O]	2.27	ARG 3[HH22]
7	LEU 46[O]	1.97	ARG 3[HH21]
8	ASP 86[OD2]	2.72	GLY 4[N]
9	ASP 86[OD2]	2.95	VAL 5[N]
10	ALA 31[O]	2.24	CYS 21[HG]
11	CYS 16[SG]	2.44	ARG 59[HH12]
12	CYS 16[SG]	2.27	ARG 59[HH22]
13	ASN 81[OD1]	3.84	GLN 122[N]

(b) Interactions between IGF1-LHβ

Hydrogen bonds			
S. No.	IGF1	Dist. [Å]	LHβ
1	SER 18[O]	2.22	ASN 31[HD21]
2	SER 135[OG]	3.11	VAL 46[N]
3	CYS 16[N]	3.15	SER 17[OG]
4	ARG 19[HE]	1.68	THR 33[OG1]
5	ARG 19[HH21]	1.62	ASP 126[OD2]
6	GLY 20[N]	3.88	ASN 31[O]
7	ARG 21[N]	3.64	GLU 32[OE2]
8	ARG 21[HH11]	1.66	GLU 32[OE1]
9	ARG 21[HH22]	2.46	ASP 126[OD2]
10	ARG 25[HH11]	2.48	GLU 32[OE2]
11	ARG 25[HH12]	2.29	GLU 32[OE2]
12	ARG 25[HH22]	2.31	CYS 52[O]
13	ARG 118[HH11]	2.28	GLU 121[OE1]
14	ARG 118[HH12]	1.67	GLU 121[OE2]
Salt bridges			
1	ARG 19[NE]	3.69	ASP 126[OD2]
2	ARG 19[NH2]	2.66	ASP 126[OD2]
3	ARG 21[NH1]	2.62	GLU 32[OE1]
4	ARG 21[NH1]	3.19	GLU 32[OE2]
5	ARG 21[NH2]	3.34	GLU 32[OE1]
6	ARG 21[NH2]	3.39	ASP 126[OD2]

Table 11. Continued.

Hydrogen bonds			
S. No.	IGF1	Dist. [Å]	LHβ
7	ARG 25[NH1]	3.47	GLU 32[OE1]
8	ARG 25[NH1]	2.71	GLU 32[OE2]
9	ARG 118[NE]	3.99	GLU 121[OE2]
10	ARG 118[NH1]	2.74	GLU 121[OE1]
11	ARG 118[NH1]	2.65	GLU 121[OE2]
12	HIS 119[NE2]	2.67	TYR 138[O]
13	HIS 134[NE2]	3.03	ASP 126[OD1]
14	HIS 134[NE2	3.97	ASP 126[OD2]

(c) Interactions between IGF1-GH

Hydrogen bonds			
S.No.	IGF1	Dist. [Å]	GH
1	ARG 25[HH11]	1.80	GLU 119[OE1]
2	ARG 25[HH22]	1.55	GLU 119[OE2]
3	CYS 16[HG]	1.54	ASP 123[OD1]
4	ASP 86[OD1]	2.92	ALA 13[N]
5	PHE 90[O]	1.84	ARG 27[HH21]
6	MET 14[O]	1.86	ARG 35[HH11]
Salt bridges			
1	ARG 25[NH1]	2.80	GLU 119[OE1]
2	ARG 25[NH2]	3.87	GLU 119[OE1]
3	ARG 25[NH1]	3.02	GLU 119[OE2]
4	ARG 25[NH2]	2.56	GLU 119[OE2]

Chrysiptera cyanea has a partial cDNA sequence containing an ORF of 600 bp encoding 155 aa (Mahardini et al. 2018). *Paralichthys adspersus* and *Platichthys stellatus*, have 558 bp long ORF encoding 185 aa and a 44 aa long signal peptide, respectively (Escobar et al. 2011; Xu et al. 2015).

The predicted molecular weight of IGF1 is 17.656 kDa and the isoelectric point (pI) is 9.92 suggests protein to be basic in nature. Our results are in accordance with that of *Labeo rohita*, wherein the predicted molecular weight (17.87241 kDa) and pI (9.10) have been reported (Roy 2017). The aliphatic index and GRAVY of IGF1-index suggests that this protein is not thermostable and is hydrophilic in nature. IGF1 has more random coils and alpha helix than extended strands and beta turns as seen in *Labeo rohita*. Beta bridges are completely absent (Roy 2017). Presence of signal peptide of 41 aa at the N-terminal region in IGF1 suggests that it is secretory in nature and extracellularly localized. Phosphorylation, post-translational modification, provides stability to the protein and helps in protein activity, localization, and transportation. Serine (S), threonine (T) and tyrosine (Y) are the main phosphorylation sites of the protein (Mittal & Saluja 2015; Suskiewicz 2024). In *H. fossilis*, maximum phosphorylation has been observed on serine residues in comparison with threonine and tyrosine residues. It is involved in biological processes like signaling pathways, metabolism regulation, and transport. IGF1 exhibits its interaction with IGF1R, estrogen receptors (ESR1 and ESR2a), GH, MAPK14b, aromatase (CYP19A1A), and other proteins, which predicts that in addition to anti-apoptotic activity it is also linked with reproduction. Protein-protein interaction helps in understanding biological phenomena like intracellular communication, apoptosis, growth and reproduction (Nooren & Thornton 2003).

Protein structures were predicted using I-TASSER depending upon the C-score and TM-score. C-score is a standard that I-TASSER uses to evaluate the predicted model quality, which is calculated on the basis of convergence parameters used for structure assembly simulations and threading template alignment significance. C-score ranging between (-5,2) are considered to be robust and reliable models. Higher C-score suggests the confidence of the model and vice-versa. The TM-score is used to estimate how similar the predicted model is to the template model. TM-score more than 0.5 suggest that the model is

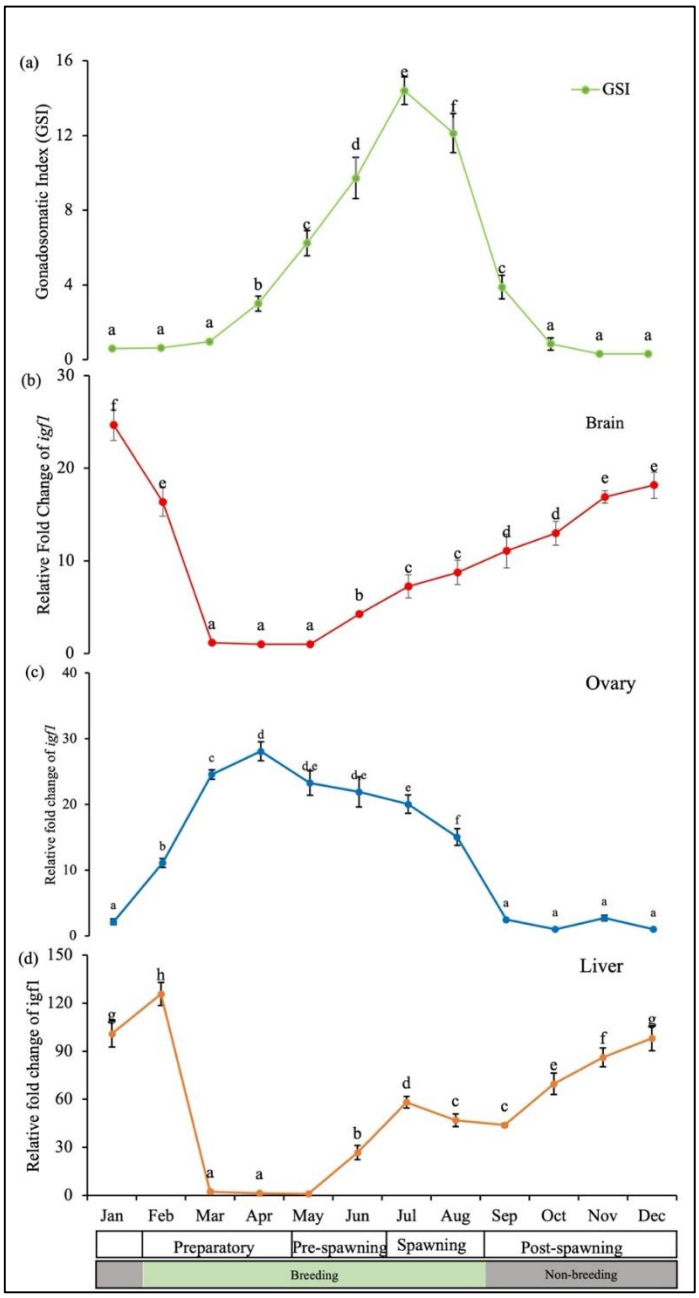

Fig.10. (a) Changes in gonadosomatic index (GSI) and relative fold change of *igf1* in (b) brain (Hypothalamus-pituitary), (c) ovary (gonadal) and (d) liver throughout the reproductive cycle of female catfish, *H. fossilis*. Values are represented as mean±SEM, (n=6). Differences in the groups are represented by different superscripts. One-way ANOVA is followed by Duncan's multiple post-hoc test.

highly reliable and has a stable topology. TM-score less than 0.17 suggests the model is made from random templates and is not considered a good model (Zhang 2008; Yang & Zhang 2015; Zheng et al. 2021; Zhou et al. 2022). All the protein models of our study fall within the range of c-score and tm-score suggesting the models are highly reliable. The models have been validated using the ERRAT scores which indicate the overall quality factor of the model for non-bonded atomic interactions. Scores greater than 50 are usually considered to be high quality models (Colovos & Yeates 1993; Messaoudi et al. 2013). WHATIF and Ramachandran z-scores are used to assess the quality of structure models and it is a standard and reliable way in structural biology and bioinformatics (Vriend 1990; Laskowski et al. 1993). The scores of protein models suggest that the models exhibit favorable stereochemical properties, stable conformational structures and adhere to the expected structural characteristics. To identify any errors in 3-D protein structures and to assess the total energy deviation of the predicted model from the energy acquired from random conformations, models were submitted to the ProSA web server (Wiederstein & Sippl 2007; Messaoudi et al. 2013). ProSA web computes the z-score, which indicates the fold reliability. Scores for the protein models suggest that the quality of predicted structures are good.

In addition to the in silico analysis, gene expression profiling of *igf1* in three tissues (brain, ovary and liver), which are integral components of HPG axis, has been undertaken and correlated with ovarian development during annual reproductive cycle. *H. fossilis* is a seasonal breeder and can be broadly divided into reproductively active phase (breeding season) and reproductively inactive phase (non-breeding season). The reproductively active breeding season involves preparatory, pre-spawning and spawning phases and reproductively inactive non-breeding season involves the post-spawning phase or quiescent phase. Gonadal recrudescence occurs during the preparatory phase which includes proliferation and growth of multiple primary oocytes leading to the formation of yolky oocytes due to incorporation of a major egg-yolk precursor protein (vitellogenin). This protein is synthesized in liver under the influence of estradiol-17β (E_2) and released into circulation immediately that finally leads to increase in ovarian weight subsequently increasing the gonadosomatic index (GSI) of *H. fossilis* (Goswami & Sundararaj 1968; Lamba et al. 1983; Pant et al.

2023). Gene expression of *igf1* in ovary is concomitant with the GSI. Transcript levels of *igf1* increases with the initiation of vitellogenesis. Upregulated expression during the preparatory phase suggests that *igf1* plays a significant role during differentiation and initial growth of primary oocytes (Berishvili et al. 2006a; Lokman et al. 2007; Yuan et al. 2018). Similar observations have been reported in zebrafish (*Danio rerio*) where the expression of *igf1* is upregulated during this stage (Zhou et al. 2016). IGF1 plays an important role in steroidogenesis by increasing the expression of ovarian aromatase enzyme (CYP19A) in granulosa cells which helps in synthesizing E_2 in fish like *Pagrus major* and *Oncorhynchus mykiss* (Steinkampf et al. 1988; Kagawa et al. 2003; Nakamura et al. 2016; Mukherjee et al. 2017).

In contrast to the ovary, gene expression of *igf1* in brain is relatively high during the early preparatory phase but reduces significantly during the mid-preparatory phase. Identical trend for gene expression of *igf1* has been observed during the preparatory phase in liver. Liver is the main site where most of the metabolic activities occur. Synthesis of vitellogenin is one of those activities during preparatory phase in oviparous catfish. Hence, with the initiation of vitellogenesis (high energy consuming process), there is a shift from somatic growth to ovarian growth (Davis et al. 2007; Rawat et al. 2013). Production of IGF1 in liver is under the influence of growth hormone therefore it also mediates the physiological functions of GH (metabolism, development, somatic growth, and cell differentiation) (Moriyama et al. 2000; Neirijnck et al. 2019). Downregulation of *igf1* expression in liver indicates the commencement of vitellogenin in response to E_2 indicating influence of E_2 on expression of *igf1*. Similar observation has been reported in many teleost where an increase in synthesis of E_2 levels suppresses the hepatic transcript level as well as the plasma level of IGF1 (Riley et al. 2002; Carnevali et al. 2005; Filby et al. 2006; Davis et al. 2007; Hanson et al. 2012; Mahardini et al. 2018). However, in immature rainbow trout, no change in transcript levels of *igf1* has been observed on treating with E_2 (Cleveland & Weber 2015).

Late pre-spawning phase is characterized by yolk-laden fully-grown oocytes with the maximum GSI. With the onset of torrential monsoon rains, fish perceives the external stimuli culminating into maturation of oocytes i.e., germinal vesicle breakdown (GVBD). A definite role of IGF1 during oocyte maturation may be assumed due to sustained expression of ovarian *igf1* and upregulation of expression of *igf1* transcripts in brain. A perusal of literature suggests direct or indirect role of ovarian *igf1* in regulating the maturation-inducing steroid (MIS) and promoting GVBD (Steinkampf et al. 1988; Maestro et al. 1997; Sarang & Lal 2005; Campbell et al. 2006; Xie et al. 2016; Das et al. 2017). Further increase in *igf1* mRNA in brain of *Chrysiptera cyanea*, during oocyte maturation has been reported (Mahardini et al. 2018). However, in *Pampus argenteus*, the expression drastically decreases in brain (Gu et al. 2021). Hepatic expression of *igf1* is upregulated during the pre-spawning phase probably indicates preparation for shift from gonadal to somatic growth.

After the release of eggs during spawning phase, ovarian weight is reduced significantly. Expression of *igf1* in ovaries is downregulated in contrast to expression of *igf1* in brain that is upregulated and attains maximum expression during the resting phase. Variations in the transcript levels of *igf1* throughout the reproductive cycle in ovary and brain suggests its involvement in steroidogenesis as well as in regulating gonadotropins. Immunoreactivity against IGF1 has been reported in purkinje cells, dendrites, and neurons of the brain of *Oreochromis niloticus* (Reinecke et al. 1997; Berishvili et al. 2006b). In *Oncorhynchus kisutch* and *Danio rerio*, pre-incubation of cultured pituitary cells with IGF1 has increased the FSH content in the culture media (Baker et al. 2000; Furukuma et al. 2008; Lin & Ge 2009). Expression of *igf1* in liver and brain during post-spawning phase suggests a shift of metabolic energy towards somatic growth from gonadal growth. Further transcription pattern of *igf1* in all the three tissues during the reproductive cycle of the catfish illustrates that *igf1*

may play an important role in ovarian growth and oocyte maturation via autocrine, paracrine and endocrine mechanisms. Further investigations are necessary to confirm whether IGF1 from neural tissue (brain) or peripheral tissue (liver) is responsible for the regulation vitellogenesis.

The present study provides a glance at the IGF1 system in *H. fossilis*. The in silico analysis indicates that not only it has anti-apoptotic properties but it is also involved in reproduction. As crystal structures are not available in the databases, three-dimensional structures have been validated. Docked complexes of IGF1-FSHβ, IGF1-LHβ, and IGF1-GH have been generated, which are suggestive of physiological functional relevance. However, in vivo experiments are required for their confirmation. Currently, there is no existing literature that shows the interacting residues among these proteins. Varying expression of *igf1* in brain, liver and ovary throughout the annual reproductive cycle of *H. fossilis* suggest its potential influence on the endocrine HPG axis. There is a clear transition from somatic to gonadal growth and vice-versa suggesting a correlation between the somatic and gonadal axes.

ACKNOWLEDGEMENT

This work was supported by Institute of Eminence (IoE), University of Delhi (Ref. no./IoE/2021/12/FRP; Dated: 31.08.2022). Uma Bharati Sahu acknowledges University Grant Commission for financial assistance and Department of Zoology, University of Delhi for providing research facilities.

REFERENCES

Arukwe, A. 2001. Cellular and molecular responses to endocrine-modulators and the impact on fish reproduction. Marine Pollution Bulletin 42(8): 643-655.

Baker, D.M.; Davies, B.; Dickhoff, W.W. & Swanson, P. 2000. Insulin-like growth factor I increases follicle-stimulating hormone (FSH) content and gonadotropin-releasing hormone-stimulated FSH release from coho salmon pituitary cells in vitro. Biology of Reproduction 63(3): 865-871.

Berishvili, G.; Baroiller, J.F.; Eppler, E. & Reinecke, M. 2010. Insulin-like growth factor-3 (IGF-3) in male and female gonads of the tilapia: Development and regulation of gene expression by growth hormone (GH) and 17α-ethinylestradiol (EE2). General and Comparative Endocrinology 167(1): 128-134.

Berishvili, G.; D'Cotta, H.; Baroiller, J.F.; Segner, H., & Reinecke, M. 2006. Differential expression of IGF-I mRNA and peptide in the male and female gonad during early development of a bony fish, the tilapia *Oreochromis niloticus*. General and Comparative Endocrinology 146(3): 204-210.

Berishvili, G.; Shved, N.; Eppler, E.; Clota, F.; Baroiller, J.F. & Reinecke, M. 2006b. Organ-specific expression of IGF-I during early development of bony fish as revealed in the tilapia, *Oreochromis niloticus*, by in situ hybridization and immunohistochemistry: indication for the particular importance of local IGF-I. Cell and Tissue Research 325(2): 287-301.

Biran, J., & Levavi-Sivan, B. 2018. Endocrine control of reproduction. Fish Encyclopedia of Reproduction pp: 362–368.

Boan, A.F.; Delgadin, T.H.; Canosa, L.F. & Fernandino, J. I. 2024. Loss of function in somatostatin receptor 5 has no impact on the growth of medaka fish due to compensation by the other paralogs. General and Comparative Endocrinology 351: 114478.

Campbell, B.; Dickey, J.; Beckman, B.; Young, G.; Pierce, A.; Fukada, H. & Swanson, P. 2006. Previtellogenic oocyte growth in salmon: relationships among body growth, plasma insulin-like growth factor-1, estradiol-17beta, follicle-stimulating hormone and expression of ovarian genes for insulin-like growth factors, steroidogenic-acute regulatory protein and receptors for gonadotropins, growth hormone, and somatolactin. Biology of Reproduction 75(1): 34-44.

Carnevali, O.; Cardinali, M.; Maradonna, F.; Parisi, M.; Olivotto, I.; Polzonetti-Magni, A.M.; Mosconi, G. & Funkenstein, B. 2005. Hormonal regulation of hepatic IGF-I and IGF-II gene expression in the marine teleost *Sparus aurata*. Molecular Reproduction and Development, 71(1): 12–18.

Chaube, R.; Sharma, S.; Senthilkumaran, B.; Bhat, S.G. & Joy, K.P. 2022. Kisspeptins stimulate the hypothalamus-pituitary-ovarian axis and induce final oocyte maturation and ovulation in female stinging catfish (*Heteropneustes fossilis*): Evidence from in vivo and in vitro studies. Aquaculture 548: 737734.

Chomczynski, P. & Sacchi, N. 2006. The single-step

method of RNA isolation by acid guanidinium thiocyanate-phenol-chloroform extraction: Twenty-something years on. Nature Protocols, 1(2): 581–585.

Cleveland, B.M. & Weber, G.M. 2015. Effects of sex steroids on expression of genes regulating growth-related mechanisms in rainbow trout (*Oncorhynchus mykiss*). General and Comparative Endocrinology 216: 103-115.

Colovos, C. & Yeates, T. O. 1993. Verification of protein structures: patterns of nonbonded atomic interactions. Protein Science 2(9): 1511-1519.

Das, D.; Khan, P.P. & Maitra, S. 2017. Endocrine and paracrine regulation of meiotic cell cycle progression in teleost oocytes: cAMP at the centre of complex intra-oocyte signalling events. General and Comparative Endocrinology 241:33-40.

Davis, L.K.; Hiramatsu, N.; Hiramatsu, K.; Reading, B.J.; Matsubara, T.; Hara, A.; Sullivan, C.V.; Pierce, A.L.; Hirano, T. & Grau, E.G. 2007. Induction of three vitellogenins by 17beta-estradiol with concurrent inhibition of the growth hormone-insulin-like growth factor 1 axis in a euryhaline teleost, the tilapia (*Oreochromis mossambicus*). Biology of Reproduction 77(4): 614-625.

Denley, A.; Cosgrove, L.J.; Booker, G.W.; Wallace, J.C. & Forbes, B.E. 2005. Molecular interactions of the IGF system. Cytokine and Growth Factor Reviews 16(4-5): 421–439.

Duan, C.; Ren, H. & Gao, S. 2010. Insulin-like growth factors (IGFs), IGF receptors, and IGF-binding proteins: Roles in skeletal muscle growth and differentiation. General and Comparative Endocrinology 167(3): 344-351.

Duan, C. & Xu, Q. 2005. Roles of insulin-like growth factor (IGF) binding proteins in regulating IGF actions. General and Comparative Endocrinology 142(1-2): 44-52.

Escobar, S.; Fuentes, E.N.; Poblete, E.; Valdés, J.A.; Safian, D.; Reyes, A.E.; Álvarez, M. & Molina, A. 2011. Molecular cloning of IGF-1 and IGF-1 receptor and their expression pattern in the Chilean flounder (*Paralichthys adspersus*). Comparative Biochemistry and Physiology - B Biochemistry and Molecular Biology 159(3): 140-147.

Filby, A.L.; Thorp, K.L. & Tyler, C.R. 2006. Multiple molecular effect pathways of an environmental oestrogen in fish. Journal of Molecular Endocrinology 37(1): 121-134.

Goswami, S.V. & Sundararaj, B. I. 1968. Compensatory hypertrophy of the remaining ovary after unilateral ovariectomy at various phases of the reproductive cycle of catfish, *Heteropneustes fossilis* (Bloch). General and Comparative Endocrinology 11(2): 401-413.

Gu, W.; Yang, Y.; Ning, C.; Wang, Y.; Hu, J.; Zhang, M.; Kuang, S.; Sun, Y.; Li, Y.; Zhang, Y.; Sun, J.; Ying, D. & Xu, S. 2021. Identification and characteristics of insulin-like growth factor system in the brain, liver, and gonad during development of a seasonal breeding teleost, *Pampus argenteus*. General and Comparative Endocrinology 300: 113645.

Hanson, A.M.; Kittilson, J.D.; McCormick, S.D. & Sheridan, M. A. 2012. Effects of 17β-estradiol, 4-nonylphenol, and β-sitosterol on the growth hormone-insulin-like growth factor system and seawater adaptation of rainbow trout (*Oncorhynchus mykiss*). Aquaculture 362: 241-247.

Hanson, S., Steeves, K., Bagatim, T., Hogan, N., Wiseman, S., Hontela, A., & Hecker, M. 2021. Health status of fathead minnow (*Pimephales promelas*) populations in a municipal wastewater effluent-dominated stream in the Canadian prairies, Wascana Creek, Saskatchewan. Aquatic Toxicology, 238: 105933.

Hara, A.; Hiramatsu, N. & Fujita, T. 2016. Vitellogenesis and choriogenesis in fishes. Fisheries science 82: 187-202.

Hober, S.; Uhlén, M. & Nilsson, B. 1997. Disulfide exchange folding of disulfide mutants of insulin-like growth factor I in vitro. Biochemistry 36(15): 4616-4622.

Hollander-Cohen, L.; Golan, M. & Levavi-Sivan, B. 2021. Differential regulation of gonadotropins as revealed by transcriptomes of distinct LH and FSH cells of fish pituitary. International Journal of Molecular Sciences 22(12): 6478.

Jones, J.I. 1995. Insulin-like growth factors and their binding proteins: biological actions. Endocrine Reviews 16(1): 3-34.

Kagawa, H.; Gen, K.; Okuzawa, K. & Tanaka, H. 2003. Effects of luteinizing hormone and follicle-stimulating hormone and insulin-like growth factor-I on aromatase activity and P450 aromatase gene expression in the ovarian follicles of red seabream, *Pagrus major*. Biology of Reproduction 68(5): 1562-1568.

Kagawa, H.; Kobayashi, M.; Hasegawa, Y. & Aida, K. 1994. Insulin and insulin-like growth factors I and II induce final maturation of oocytes of red seabream,

Pagrus major, in vitro. General and Comparative Endocrinology 95(2): 293-300.

Krieger, E.; Joo, K.; Lee, J.; Lee, J.; Raman, S.; Thompson, J. & Karplus, K. 2009. Improving physical realism, stereochemistry, and side-chain accuracy in homology modeling: four approaches that performed well in CASP8. Proteins: Structure, Function, and Bioinformatics 77(S9): 114-122.

Kumari, P.; Kumar, M.; Sehgal, N. & Aggarwal, N. 2020. In silico analysis of kiss2, expression studies and protein–protein interaction with gonadotropin-releasing hormone 2 (GnRH2) and luteinizing hormone beta (LHβ) in *Heteropneustes fossilis*. Journal of Biomolecular Structure and Dynamics 40(10): 4543–4557.

Kumari, P.; Sehgal, N.; Goswami, S.V. & Aggarwal, N. 2021. Multifactorial control of gonadotropin release for induction of oocyte maturation: Influence of gonadotropin-releasing hormone, gonadotropin release-inhibiting factor and dopamine receptors in the catfish, *Heteropneustes fossilis*. Journal of Applied and Natural Science 13(2): 686-699.

Lamba, V.J.; Goswami, S.V. & Sundararaj, B.I. 1983. Circannual and circadian variations in plasma levels of steroids (cortisol, estradiol-17β estrone, and testosterone) correlated with the annual gonadal cycle in the catfish, *Heteropneustes fossilis* (Bloch). General and Comparative Endocrinology 50(2): 205-225.

Laskowski, R.A.; MacArthur, M.W.; Moss, D.S. & Thornton, J.M. 1993. PROCHECK: a program to check the stereochemical quality of protein structures. Journal of Applied Crystallography 26(2): 283-291.

Le Roith, D.; Bondy, C.; Yakar, S.; Liu, J.L. & Butler, A. 2001. The somatomedin hypothesis: 2001. Endocrine Reviews 22(1): 53-74.

Levavi-Sivan, B.; Bogerd, J.; Mañanós, E.L.; Gómez, A. & Lareyre, J.J. 2010. Perspectives on fish gonadotropins and their receptors. General and Comparative Endocrinology 165(3): 412-437.

Li, J.; Liu, Z.; Kang, T.; Li, M.; Wang, D. & Cheng, C.H. 2021. Igf3: a novel player in fish reproduction. Biology of Reproduction, 104(6): 1194-1204.

Lin, S.W. & Ge, W. 2009. Differential regulation of gonadotropins (FSH and LH) and growth hormone (GH) by neuroendocrine, endocrine, and paracrine factors in the zebrafish-An in vitro approach. General and Comparative Endocrinology 160(2): 183-193.

Liu, H.; Guo, Q.; Zhang, L.; Tian, X.; Ma, X.; Zhang, J.X. & Li, X. 2022. The insulin-like growth factor 1 stimulates ovarian steroidogenesis and oocyte maturation in spotted steed *Hemibarbus maculatus*. Journal of Steroid Biochemistry and Molecular Biology 224: 106159.

Livak, K.J. & Schmittgen, T.D. 2001. Analysis of relative gene expression data using real-time quantitative PCR and the 2-ΔΔCT method. Methods 25(4): 402-408.

Lokman, P.M.; George, K.A.N.; Divers, S.L.; Algie, M. & Young, G. 2007. 11-Ketotestosterone and IGF-I increse the size of previttelogenic oocytes from shortfinned eel, *Anguilla australis*, in vitro. Reproduction 133(5): 955-967.

Lubzens, E.; Young, G.; Bobe, J. & Cerdà, J. 2010. Oogenesis in teleosts: How fish eggs are formed. General and Comparative Endocrinology 165(3): 367-389.

Luckenbach, J.A.; Dickey, J.T. & Swanson, P. 2010. Regulation of pituitary GnRH receptor and gonadotropin subunits by IGF1 and GnRH in prepubertal male coho salmon. General and Comparative Endocrinology 167(3): 387-396.

Maestro, M.A.; Planas, J.V.; Moriyama, S.; Gutiérrez, J.; Planas, J. & Swanson, P. 1997. Ovarian receptors for insulin and insulin-like growth factor I (IGF-I) and effects of IGF-I on steroid production by isolated follicular layers of the preovulatory coho salmon ovarian follicle. General and Comparative Endocrinology 106(2): 189-201.

Magee, B.A.; Shooter, G.K.; Wallace, J. C. & Francis, G. L. 1999. Insulin-like growth factor I and its binding proteins: A study of the binding interface using B-domain analogues. Biochemistry 38(48): 15863-15870.

Mahardini, A.; Yamauchi, C.; Takeuchi, Y.; Rizky, D.; Takekata, H. & Takemura, A. 2018. Changes in mRNA abundance of insulin-like growth factors in the brain and liver of a tropical damselfish, *Chrysiptera cyanea*, in relation to seasonal and food-manipulated reproduction. General and Comparative Endocrinology 269: 112-121.

Mcbride, R.S.; Somarakis, S.; Fitzhugh, G.R.; Albert, A.; Yaragina, N.A.; Wuenschel, M.J.; Alonso-Fernández, A. & Basilone, G. 2015. Energy acquisition and allocation to egg production in relation to fish reproductive strategies. Fish and Fisheries 16(1): 23-57.

Messaoudi, A.; Belguith, H. & Ben Hamida, J. 2013. Homology modeling and virtual screening approaches to identify potent inhibitors of VEB-1 β-lactamase.

Theoretical Biology and Medical Modelling 10: 1-10.

Mittal, S., Saluja, D. 2015. Protein Post-translational Modifications: Role in Protein Structure, Function and Stability. In: Singh, L.R., Dar, T.A., Ahmad, P. (eds) Proteostasis and Chaperone Surveillance. Springer, New Delhi.

Moriyama, S.; Ayson, F.G. & Kawauchi, H. 2000. Growth regulation by insulin-like growth factor-1 in fish. Bioscience, Biotechnology and Biochemistry 64(8): 1553-1562.

Mukherjee, D., Majumder, S., Moulik, S. R., Pal, P., Gupta, S., Guha, P., & Kumar, D. 2017. Membrane receptor cross talk in gonadotropin-, IGF-I, and insulin-mediated steroidogenesis in fish ovary: an overview. General and Comparative Endocrinology 240: 10-18.

Nagahama, Y. & Yamashita, M. 2008. Regulation of oocyte maturation in fish. Development, growth and differentiation 50: S195-S219.

Nakamura, I.; Kusakabe, M.; Swanson, P. & Young, G. 2016. Regulation of sex steroid production and mRNAs encoding gonadotropin receptors and steroidogenic proteins by gonadotropins, cyclic AMP and insulin-like growth factor-I in ovarian follicles of rainbow trout (*Oncorhynchus mykiss*) at two stages of vitellogenesis. Comparative Biochemistry and Physiology Part A: Molecular & Integrative Physiology 201: 132-140.

Ndandala, C.B.; Dai, M.; Mustapha, U.F.; Li, X.; Liu, J.; Huang, H. & Chen, H. 2022. Current research and future perspectives of GH and IGFs family genes in somatic growth and reproduction of teleost fish. Aquaculture Reports 26: 101289.

Negatu, Z.; Hsiao, S.M. & Wallace, R.A. 1998. Effects of Insulin-like Growth Factor-I on Final Oocyte Maturation and Steroid Production in *Fundulus Heteroclitus*. Fish Physiology and Biochemistry 19: 13-21.

Neirijnck, Y.; Papaioannou, M.D. & Nef, S. 2019. The insulin/IGF system in mammalian sexual development and reproduction. International Journal of Molecular Sciences 20(18): 4440.

Nipkow, M.; Wirthgen, E.; Luft, P.; Rebl, A.; Hoeflich, A. & Goldammer, T. 2018. Characterization of *igf1* and *igf2* genes during maraena whitefish (*Coregonus maraena*) ontogeny and the effect of temperature on embryogenesis and *igf* expression. Growth Hormone & IGF Research 40: 32-43.

Nooren, I.M.A. & Thornton, J.M. 2003. Structural characterisation and functional significance of transient protein-protein interactions. Journal of Molecular Biology, 325(5): 991-1018.

Pant, D.R.; Ila, K.; Sahu, U.B. & Sehgal, N. 2023. Temporal expression of thyroid hormone regulating genes (tsh-b, tsh-r, dio2 and dio3) and their correlation with annual reproductive cycle of the Indian freshwater catfish, *Heteropneustes fossilis* (Bloch). Journal of Applied and Natural Science 15(1): 41-56.

Philippou, A.; Maridaki, M.; Pneumaticos, S. & Koutsilieris, M. 2014. The complexity of the IGF1 gene splicing, posttranslational modification and bioactivity. Molecular Medicine, 20: 202-214.

Pipil, S., Kumar, V., Rawat, V. S., Sharma, L., & Sehgal, N. 2015. In silico and in vivo analysis of binding affinity of estrogens with estrogen receptor alpha in *Channa punctatus* (Bloch). Fish Physiology and Biochemistry, 41: 31–40.

Qin, Q.; Chen, X.; Zhu, X.; Li, X.; Zhao, Y.; Xu, Z. & Liu, W. 2020. Insulin-like growth factor I of Yellow catfish (*Pelteobagrus fulvidraco*): cDNA characterization, tissue distribution, and expressions in response to starvation and refeeding. Fish Physiology and Biochemistry 46: 177-186.

Rawat, V.S.; Rani, K.V.; Phartyal, R. & Sehgal, N. 2013. Vitellogenin genes in fish: Differential expression on exposure to estradiol. Fish Physiology and Biochemistry, 39: 39–46.

Reinecke, M. 2010. Insulin-like growth factors and fish reproduction. Biology of Reproduction 82(4): 656-661.

Reinecke, M.; Björnsson, B.T.; Dickhoff, W.W.; McCormick, S.D.; Navarro, I.; Power, D.M. & Gutiérrez, J. 2005. Growth hormone and insulin-like growth factors in fish: Where we are and where to go. General and Comparative Endocrinology 142(1-2): 20-24.

Reinecke, M.; Schmid, A.; Ermatinger, R. & Loffing-Cueni, D. 1997. Insulin-like growth factor I in the teleost *Oreochromis mossambicus*, the tilapia: Gene sequence, tissue expression, and cellular localization. Endocrinology 138(9): 3613-3619.

Riley, L.G.; Hirano, T. & Grau, E.G. 2002. Disparate effects of gonadal steroid hormones on plasma and liver mRNA levels of insulin-like growth factor-I and vitellogenin in the tilapia, *Oreochromis mossambicus*. Fish Physiology and Biochemistry 26: 223-230.

Roy, A.K. 2017. Analysis of Insulin-Like Growth Factor I and Its Receptor of an Indian Major Carp *Labeo rohita*: An In silico Approach. MOJ Proteomics &

Bioinformatics 6(3): 00195.

Roy, A.; Kucukural, A. & Zhang, Y. 2010. I-TASSER: A unified platform for automated protein structure and function prediction. Nature Protocols 5(4): 725-738.

Sarang, M. K., & Lal, B. 2005. Effect of piscine GH/IGF-I on final oocyte maturation in vitro in *Heteropneustes fossilis*. Fish Physiology and Biochemistry 31: 231-233.

Steinkampf, M.P.; Mendelson, C.R. & Simpson, E.R. 1988. Effects of epidermal growth factor and insulin-like growth factor I on the levels of mRNA encoding aromatase cytochrome P-450 of human ovarian granulosa cells. Molecular and Cellular Endocrinology, 59(1-2): 93-99.

Suskiewicz, M. J. 2024. The logic of protein post-translational modifications (PTMs): Chemistry, mechanisms and evolution of protein regulation through covalent attachments. BioEssays 46(3): 2300178.

Torre, S.; Della Benedusi, V.; Fontana, R. & Maggi, A. 2014. Energy metabolism and fertility - A balance preserved for female health. Nature Reviews Endocrinology 10(1): 13-23.

Triantaphyllopoulos, K.A.; Cartas, D. & Miliou, H. 2020. Factors influencing GH and IGF-I gene expression on growth in teleost fish: how can aquaculture industry benefit?. Reviews in Aquaculture 12(3): 1637-1662.

Vasal, S. & Sundararaj, B.I. 1976. Response of the ovary in the catfish, *Heteropneustes fossilis* (Bloch), to various combinations of photoperiod and temperature. Journal of Experimental Zoology 197(2): 247-263.

Vriend, G. 1990. WHAT IF: A molecular modeling and drug design program. Journal of Molecular Graphics 8(1): 52-56.

Wang, D.S.; Jiao, B.; Hu, C.; Huang, X.; Liu, Z. & Cheng, C.H.K. 2008. Discovery of a gonad-specific IGF subtype in teleost. Biochemical and Biophysical Research Communications 367(2): 336-341.

Weil, C.; Carré, F.; Blaise, O.; Breton, B. & Le Bail, P.Y. 1999. Differential effect of insulin-like growth factor I on in vitro gonadotropin (I and II) and growth hormone secretions in rainbow trout (*Oncorhynchus mykiss*) at different stages of the reproductive cycle. Endocrinology 140(5): 2054-2062.

Wiederstein, M. & Sippl, M.J. 2007. ProSA-web: Interactive web service for the recognition of errors in three-dimensional structures of proteins. Nucleic Acids Research 35(Suppl_2): W407-W410.

Wood, A.W.; Duan, C. & Bern, H.A. 2005. Insulin-like growth factor signaling in fish. International Review of Cytology 243(1): 215-285.

Xie, L.; Tang, Q.; Yang, L. & Chen, L. 2016. Insulin-like growth factor I promotes oocyte maturation through increasing the expression and phosphorylation of epidermal growth factor receptor in the zebrafish ovary. Molecular and Cellular Endocrinology 419: 198-207.

Xu, Y.; Zang, K.; Liu, X.; Shi, B.; Li, C. & Shi, X. 2015. Insulin-like growth factors I and II in starry flounder (*Platichthys stellatus*): molecular cloning and differential expression during embryonic development. Fish Physiology and Biochemistry 41: 139-152.

Yang, J. & Zhang, Y. 2015. I-TASSER server: New development for protein structure and function predictions. Nucleic Acids Research 43(W1): W174-W181.

Yuan, C.; Chen, K.; Zhu, Y.; Yuan, Y. & Li, M. 2018. Medaka igf1 identifies somatic cells and meiotic germ cells of both sexes. Gene 642: 423-429.

Zhang, Y. 2008. I-TASSER server for protein 3D structure prediction. BMC Bioinformatics 9(40): 1-8.

Zheng, W.; Zhang, C.; Li, Y.; Pearce, R.; Bell, E.W. & Zhang, Y. 2021. Folding non-homologous proteins by coupling deep-learning contact maps with I-TASSER assembly simulations. Cell Reports Methods 1(3): 100014.

Zhou, R.; Yu, S.M.Y.; & Ge, W. 2016. Expression and functional characterization of intrafollicular GH–IGF system in the zebrafish ovary. General and Comparative Endocrinology 232: 32-42.

Zhou, X.; Zheng, W.; Li, Y.; Pearce, R.; Zhang, C.; Bell, E.W.; Zhang, G. & Zhang, Y. 2022. I-TASSER-MTD: a deep-learning-based platform for multi-domain protein structure and function prediction. Nature Protocols 17(10): 2326-2353.

Zohar, Y.; Muñoz-Cueto, J.A.; Elizur, A. & Kah, O. 2010. Neuroendocrinology of reproduction in teleost fish. General and Comparative Endocrinology 165(3): 438-455.

Iran. J. Ichthyol. (2024) 11(2): 124-146
P-ISSN: 2383-1561; E-ISSN: 2383-0964
http://www.ijichthyol.org

doi: 10.22034/iji.v11i2.1006

مقاله کامل

فاکتور رشد شبه انسولین ۱ (IGF1) در محور هیپوتالاموس-هیپوفیز-گناد-کبد (HPG-L): شناسایی، توالی‌یابی، بیان ژن و در تجزیه و تحلیل سیلیکو در گربه ماهی آب شیرین هند، *Heteropneustes fossilis*

یوما باراتی[۱]، کوماری وانداانا رانی[۲]، نیتا سیگال*[۱]

[۱]گروه جانورشناسی، دانشگاه دهلی، دهلی، هند.

[۲]گروه جانورشناسی، کالج کالیندی، دانشگاه دهلی، دهلی، هند.

چکیده: فاکتور رشد شبه انسولین ۱ (IGF1) در عملکردهای فیزیولوژیکی مختلفی که توسط محور سوماتوتروپیک (GH-IGF1) تنظیم می شوند، دخالت دارد. برای رمزگشایی نقش IGF1 در ژن محور HPG-L کد کننده cDNA igf1 گربه ماهی ماده، *Heteropneustes fossilis*، به‌دنبال آن در تجزیه و تحلیل سیلیکو و همچنین بیان فصلی igf1 در مغز، کبد و اندام‌های تخمدان توالی‌یابی شده است. بیان mRNA ژن igf1 در این سه اندام نشان می‌دهد که نقش اساسی در محور HPG-L ایفا می کند. در تخمدان، بیان ژن igf1 ارتباط مستقیمی با شاخص گنادوسوماتیک نشان می‌دهد، در حالی که یک رابطه معکوس در بافت مغز و کبد مشاهده شده است. از این رو تنظیم مثبت igf1 در مغز و کبد، در مرحله پس از تخم‌ریزی و کاهش در تخمدان، تغییر از رشد غدد جنسی به رشد جسمی در فاز استراحت را نشان می‌دهد. در تجزیه و تحلیل سیلیکو نشان می‌دهد که IGF1 دارای خاصیت پایدار و آبدوست با ۱۵۹ اسید آمینه (aa) و وزن مولکولی ۱۷/۶۵ کیلو دالتون است. ساختار ثانویه حضور حداکثر پیچش‌های نامنظم و مارپیچ-آلفا را نشان می‌دهد. این پروتئین ترشحی است که بیشترین تعامل را با IGF1R، گیرنده استروژن آلفا و GH نشان می‌دهد. ساختارهای پروتئینی IGF1، هورمون لوتئولین بتا (LHβ)، هورمون محرک فولیکول بتا (FSHβ) و هورمون رشد (GH) ساخته شده‌اند و برهمکنش بین آنها ثابت شده است که نشان می‌دهد احتمالاً محورهای غدد جنسی و جسمی به هم مرتبط هستند و ممکن است نوروآندوکرین سیستم ماهی را تنظیم کنند.

کلمات‌کلیدی: فاکتور رشد شبه انسولین ۱ (IGF1)، آنالیز سیلیکو، محور هیپوتالاموس-هیپوفیز-گناد-کبد (HPG-L)، تولیدمثل فصلی، *Heteropneustes fossilis*.